CrossMark

ORIGINAL ARTICLE

Integrated PET/MRI for whole-body staging of patients with primary cervical cancer: preliminary results

Johannes Grueneisen[1] · Benedikt Michael Schaarschmidt[2] · Martin Heubner[3] ·
Bahriye Aktas[3] · Sonja Kinner[1] · Michael Forsting[1] · Thomas Lauenstein[1] ·
Verena Ruhlmann[4] · Lale Umutlu[1]

Abstract

Purpose To assess the diagnostic value of integrated PET/
MRI for whole-body staging of cervical cancer patients, as
well as to investigate a potential association between PET/
MRI derived functional parameters and prognostic factors of
cervical cancer.

Methods The present study was approved by the local institutional review board. Twenty-seven patients with histopathologically confirmed cervical cancer were prospectively enrolled in our study. All patients underwent a whole-body PET/MRI examination after written informed consent was obtained. Two radiologists separately evaluated the PET/MRI data sets regarding the determination of local tumor extent of primary cervical cancer lesions, as well as detection of nodal and distant metastases. Furthermore, SUV and ADC values of primary tumor lesions were analyzed and correlated with dedicated prognostic factors of cervical cancer. Results based on histopathology and cross-sectional imaging follow-up served as the reference standard.

Results PET/MRI enabled the detection of all 27 primary tumor lesions of the uterine cervix and allowed for the correct determination of the T-stage in 23 (85 %) out of the 27 patients. Furthermore, the calculated sensitivity, specificity and diagnostic accuracy for the detection of nodal positive patients (n=11) were 91 %, 94 % and 93 %, respectively. PET/MRI correctly identified regional metastatic disease (N1-stage) in 8/10 (80 %) patients and non-regional lymph node metastases in 5/5 (100 %) patients. In addition, quantitative analysis of PET and MRI derived functional parameters (SUV; ADC values) revealed a significant correlation with pathological grade and tumor size (p<0.05).

Conclusions The present study demonstrates the high potential of integrated PET/MRI for the assessment of primary tumor and the detection of lymph node metastases in patients with cervical cancer. Providing additional prognostic information, PET/MRI may serve as a valuable diagnostic tool for cervical cancer patients in a pretreatment setting.

✉ Johannes Grueneisen
johannes.grueneisen@uk-essen.de

1 Department of Diagnostic and Interventional Radiology and Neuroradiology, University Hospital Essen, University of Duisburg-Essen, Hufelandstrasse 55, 45147 Essen, Germany

2 Department of Diagnostic and Interventional Radiology, University Hospital Dusseldorf, University of Dusseldorf, D-40225 Dusseldorf, Germany

3 Department of Obstetrics and Gynecology, University Hospital Essen, University of Duisburg-Essen, D-45147 Essen, Germany

4 Department of Nuclear Medicine, University Hospital Essen, University of Duisburg-Essen, D-45147 Essen, Germany

Introduction

Cervical cancer is one of the most common gynecological malignancies and the fourth most frequent cause of cancer death in women worldwide [1]. As survival rates are highly dependent on local tumor extent and potential metastatic spread at time of diagnosis, accurate staging of cervical cancer patients is needed to ensure appropriate treatment planning and predict prognosis. According to recommendations of the International Federation of Gynecology and Obstetrics (FIGO), primary tumor staging of cervical cancers is based

on clinical evaluation [2]. However, remarkable discrepancies have been reported between surgical/histological findings and corresponding tumor stages based on conventional clinical staging techniques [3, 4]. Due to its excellent soft-tissue contrast, magnetic resonance imaging (MRI) is increasingly applied for the pretherapeutic assessment of local spread of tumors of the female pelvis, while positron emission tomography (PET) has been demonstrated very accurate for the identification of metastatic spread, based on enhanced metabolic activity of tumor lesions [5, 6]. In combining morphological and functional datasets, hybrid imaging techniques such as positron emission tomography/computed tomography (PET/CT) have been shown to be highly accurate for whole-body staging in numerous solid tumor entities [7, 8]. However, CT is known to be restricted for assessment of potential tumor infiltration into surrounding tissue and assessment of local tumor spread based on its low soft-tissue contrast. Hence, the recent introduction of integrated PET/MRI systems has demonstrated its strong diagnostic potential for a high-quality diagnostic work-up, combining high soft-tissue contrast, high-resolution morphological information based on MRI with metabolic data derived from the PET component [9, 10]. Furthermore, integrated PET/MRI provides the basis for a simultaneous acquisition of MRI and PET-derived functional parameters [11]. Although the standardized uptake value (SUV) and apparent diffusion coefficient (ADC) reflect different aspects of tumor biology, both parameters have been proven useful for treatment monitoring, as well as the prediction of tumor recurrences and clinical outcome [12–14].

Therefore, the aim of our study was to evaluate the diagnostic capability of integrated PET/MRI for whole-body tumor staging of patients with primary cervical cancer. Furthermore, we investigated a potential association of PET/MRI derived functional parameters with important prognostic factors and histology of cervical tumors.

Material and methods

Patients

The study was conducted in accordance with all guidelines set forth by the approving institutional review board, and written informed consent was obtained from all participants before each examination. Twenty-seven consecutive patients (mean age 48±12 years [28–73 years]) with primary cervical cancer were prospectively enrolled in our study. Inclusion criteria were histopathological confirmation of a primary cervical cancer. PET/MRI examinations were performed before pelvic and/or para-aortic lymphadenectomy, which was followed by definitive treatment.

PET/MRI

Whole-body PET/MRI examinations were obtained on a Magnetom Biograph mMR™ (Siemens Healthcare, Erlangen, Germany), containing LSO-based avalanche photodiodes for PET-measurements. All patients fasted for at least 6 h prior to each PET/MRI examination and exhibited blood glucose levels below 150 mg/dl. A body-weight adapted dosage (2 MBq/kg bodyweight) of 18F-fluorodeoxyglucose (18F-FDG) was injected intravenously before the scan. PET/MRI examinations were performed with an average delay of 73± 23 min after the application of 18F-FDG, exhibiting a mean activity of 143±36 MBq. PET scans were obtained with a field of view (FoV) containing the body volume from skull-base to mid-thighs. PET images were subsequently reconstructed, using the iterative ordered-subset expectation maximization algorithm, three iterations and 21 subsets, a Gaussian filter with 4.0 mm full width at half maximum and a 344×344 image matrix. Attenuation correction was performed automatically based on a four-compartment-model attenuation map (μ-map) calculated from fat-only and water-only data sets, as obtained by Dixon-based sequences. A dedicated mMR head and neck coil and phased-array body surface coils were used for MR imaging. MR data acquisition was performed simultaneously to PET imaging. The estimated examination time of whole-body PET/MR imaging amounted to 46±5 min (including shimming, contrast media administration and breath-hold commands), and comprised the following sequence protocol:

1. A coronal three-dimensional volume interpolated breath-hold examination (VIBE) sequence,
2. A transverse diffusion-weighted echo-planar imaging (EPI) sequence,
3. A coronal two-dimensional turbo inversion recovery magnitude (TIRM) sequence,
4. A fat-saturated transversal two-dimensional half-Fourier acquisition single-shot turbo spin-echo (HASTE) sequence,
5. *Pelvis only:*
   A transversal three-dimensional VIBE sequence,
6. *Pelvis only:*
   A fat-saturated sagittal three-dimensional VIBE sequence.

   For dynamic imaging, three repetitive scans were acquired with a delay of 20, 60 and 90 s after the application of i.v. contrast agent (0.1 mmol/kg bodyweight Gadobutrol, Bayer Healthcare, Germany).
7. *Pelvis only:*
   A sagittal T2-weighted (w) turbo-spin echo (TSE) sequence,
8. A post-contrast fat-saturated transversal whole-body three-dimensional VIBE sequence.

Table 1 gives detailed information for all sequences of our study protocol.

Image interpretation

Readings of PET/MRI data sets were performed by two radiologists with 5 and 6 years of experience in reading MRI and hybrid imaging, respectively, using a dedicated viewing software for hybrid imaging (Syngo.via; Siemens, Healthcare, Erlangen, Germany). Both readers were blinded to the patients' identification data and diagnosis, and analyzed the images separately in random order.

First, the readers were instructed to identify all tumor lesions, while malignancy was considered according to the following criteria: local invasion/destruction of primary tumors and distant metastases, distinctive contrast enhancement, central necrosis, short-axis nodal diameter >10 mm, nodal shape (smooth versus irregular) and focally increased FDG-uptake. Diffusion restriction was considered malignant in cases of high signal intensity in DWI images (b-1000 s/mm^2) and low signal in the corresponding ADC maps. For lesion-based analysis on integrated PET/MR images, an increased focal FDG accumulation greater than in surrounding tissue was considered as a sign of malignancy. In accordance with previous publications [15, 16], PET was considered superior, thus, morphologically suspicious and unsuspicious lesions (e.g., lymph nodes < 10 mm in short axis) were deemed positive for malignancy if a focally increased glucose uptake was detectable.

Furthermore, both readers were asked to determine the T-stage and the occurrence of potential lymph node metastases for each patient. Accordingly, potential infiltrations in the adjacent anatomical structures of the female pelvis as well as the occurrence of distant metastases were assessed.

To investigate a potential association between SUV, ADC values and prognostic factors of cervical cancer patients, an ADC map was generated by the scanner software (syngo MR B18P, Siemens, Erlangen, Germany) using three b-values (b-0, b-500, b-1000 s/mm^2). Primary cervical cancer lesions were identified on diffusion-weighted sequences (b-0), and a polygonal region of interest (ROI) was manually drawn on every slice covering the entire target lesion. After automatic transfer on the corresponding parameter map and visual confirmation of a correct placement, ADC values were determined.

For SUV measurements, tumor margins of all primary cancer lesions were identified on T1-weighted images and a polygonal volume of interest (VOI) was placed on fused PET/MR images. Mean values were calculated for each rating scale.

Reference standard

Histopathological confirmation of primary cervical cancer was available for all 27 patients included in our study. Determination of the primary tumor extent was based on histopathological correlation in patients who underwent surgical treatment ($n=20$). For the remaining seven patients, primarily treated with chemotherapy ($n=3$), or chemoradiotherapy ($n=4$), two experienced radiologists performed a consensus reading and took into account PET/MRI examinations, as well as the results of physical examination and conventional imaging. For nodal staging, histopathological findings after lymphadenectomy, as well as imaging follow-up with a focus on treatment induced-changes, were used as the reference standard.

Statistical analysis

Statistical analysis was performed using IBM SPSS version 21 (SPSS Inc, Armonk, NY, USA). Data are presented as mean values±standard deviation (SD). Mann–Whitney-U test was applied to assess statistical differences for variations in

Table 1 MR imaging parameters

	Slice thickness (mm)	Repetition time/ Echo time (ms)	Flip angle (°)	Field of view (mm)	Phase FoV (%)	Phase FoV	Parallel imaging Acceleration factor
T1w VIBE Dixon cor.	3.12	3.6 / 1.23 (1st) and 2.46 (2nd)	10	500	65.6	192×79	n / a
DW EPI (b-values: 0, 500, 1000 s/mm2) ax.	5	9900/82	90	420	75	160×90	2
T2w TIRM cor.	5	3190/55	60	450	75	384×216	2
T2w HASTE ax.	5	1500/117	160	450	81.3	320×211	2
T1w VIBE ax. (pelvis only)	2.5	5.03/2.46	9	300	68.8	512×230	2
T2w TSE sag. (pelvis only)	4	4400/101	150	280	71.9	512×221	2
T1w VIBE dynamic ax. (pelvis only)	2.5	4.46/1.71	9	300	68.8	512×246	2
T1w VIBE ax. post contrast	3.5	4.08/1.51	9	400	75	512×230	2

SUV and ADC values of primary tumor lesions based on prognostic factors of cervical cancer. A p value<0.05 was considered to indicate statistical significance. The sensitivity, specificity and diagnostic accuracy of PET/MRI for the identification of nodal positive patients was calculated. Descriptive analysis was used to present the resulting data concerning determination of the tumor stage and nodal status of all patients.

Results

Patients

PET/MRI data acquisition was completed successfully in all 27 patients without any relevant side effects. Integrated PET/MRI examinations allowed for a correct identification of all primary tumors of the uterine cervix. Tumor characteristics of all patients are presented in Table 2.

Primary tumors

Based on our reference standard the T-stage was determined for each patient and revealed 13 patients with stage IB, 4 with stage IIA, 3 with stage IIB and 5 patients with stage IIIB. Two additional patients were staged as IVA due to a histopathologically confirmed infiltration into the urinary bladder (Fig. 1). PET/MRI enabled a correct identification of the T-stage in 23 (85 %) out of the 27 patients. Two out of the remaining 4 patients were misclassified as IB according to PET/MRI, while histopathology revealed stage IIA based on local and microscopic infiltration of the surgical margins involving the vaginal cuff, not visible in PET/MRI. One IIB tumor was incorrectly classified as IIA because tumor invasion into the parametria could not be detected in PET/MRI. One further patient with tumor stage IB was misclassified as IIB based on incorrect assumption of parametrial invasion in PET/MRI ratings (see Table 3 for further details).

Table 2 Tumor characteristics and nodal status of all patients

| Patient	Histology	Tumor grade	T-stage	N-stage	M-stage
1	Squamous cell carcinoma	G3	IIB	N0	M1
2	Squamous cell carcinoma	G3	IV	N1	M1
3	Squamous cell carcinoma	G2	IB	N0	M0
4	Squamous cell carcinoma	G3	IB	N0	M0
5	Squamous cell carcinoma	G2	IB	N0	M0
6	Squamous cell carcinoma	G2	IB	N0	M0
7	Adenocarcinoma	G3	IIIB	N1	M0
8	Squamous cell carcinoma	G2	IIA	N1	M1
9	Squamous cell carcinoma	G2	IV	N0	M0
10	Adenocarcinoma	G2	IB	N0	M0
11	Squamous cell carcinoma	G2	IB	N0	M0
12	Squamous cell carcinoma	G2	IIIB	N1	M1
13	Squamous cell carcinoma	G3	IB	N1	M0
14	Adenocarcinoma	G1	IIA	N0	M0
15	Squamous cell carcinoma	G3	IIA	N0	M0
16	Squamous cell carcinoma	G3	IIIB	N1	M0
17	Squamous cell carcinoma	G3	IIIB	N1	M0
18	Squamous cell carcinoma	G2	IB	N0	M0
19	Squamous cell carcinoma	G2	IIB	N1	M0
20	Squamous cell carcinoma	G1	IB	N0	M0
21	Adenocarcinoma	G3	IIA	N0	M0
22	Squamous cell carcinoma	G2	IB	N0	M0
23	Squamous cell carcinoma	G2	IB	N1	M0
24	Squamous cell carcinoma	G2	IB	N0	M0
25	Squamous cell carcinoma	G3	IIIB	N1	M1
26	Adenocarcinoma	G2	IIB	N0	M0
27	Squamous cell carcinoma	G2	IB	N0	M0
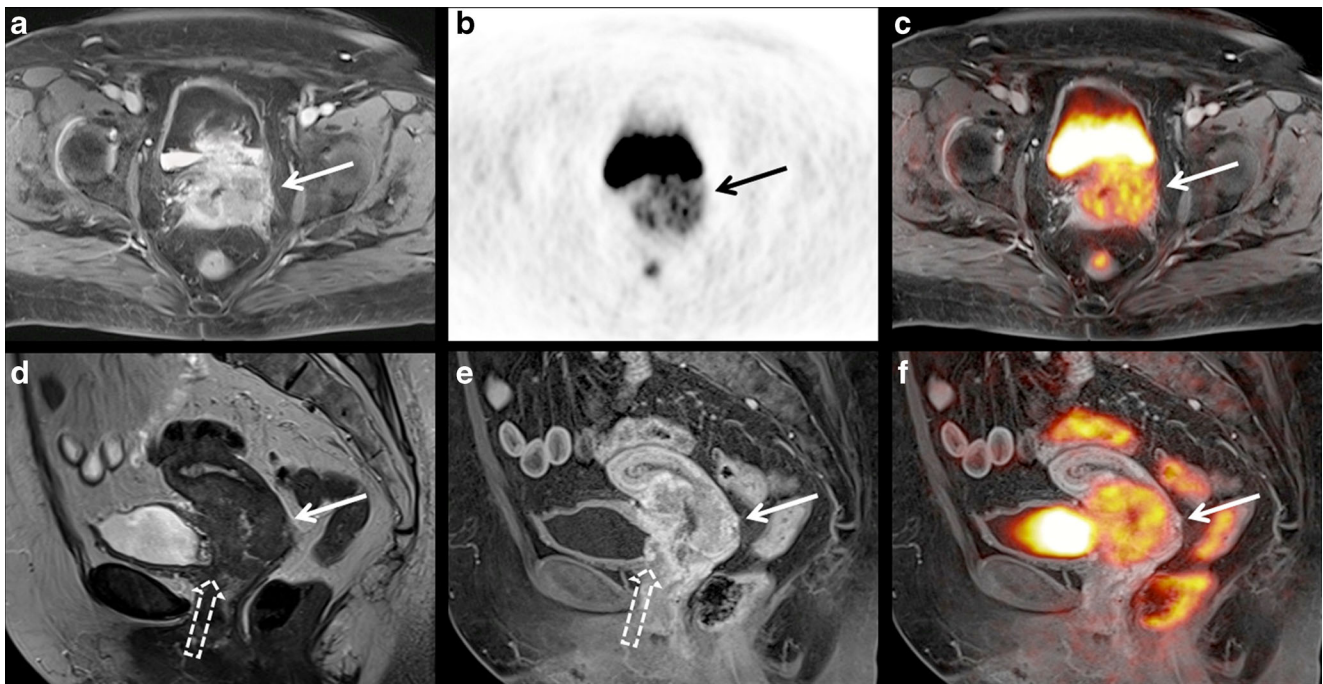
Fig. 1 Figure **a** shows an axial T1w VIBE image of an inhomogeneously contrast-enhancing tumor lesion of the uterine cervix of a 73-year-old woman (stage IVa). Elevated FDG-uptake is demonstrated on corresponding PET (**b**) and on fused PET/MR images (**c**). Corresponding sagittal imaging of the above named cervical cancer mass [T2w TSE imaging (**d**), dynamic T1w VIBE imaging (**e**) and fused PET/MR images (**f**)] show tumor invasion of the cervical mass (*arrows*) into the posterior wall of the urinary bladder (*dashed arrows*)

Assessment of metastatic disease

According to our reference standard, lymph node metastases were present in 11 (41 %) out of 27 patients (Fig. 2). PET/MRI enabled correct identification of 10/11 node-positive patients which resulted in a sensitivity of 91 % (95 % CI 59–100 %), specificity of 94 % (95 % CI 70–100 %) and diagnostic accuracy of 93 % (95 % CI 76–99 %), respectively. In one patient, PET/MRI ratings were false-positive, as one morphologically unsuspicious lymph node revealed an elevated tracer uptake as well as increased signal intensity in DWI (b-1000) and was concordantly rated as malignant. The patient was considered as node-negative after lymphadenectomy. Furthermore, regional lymph node metastases (defined as N1-stage) were found in 10 of the 11 node-positive patients. Analysis of PET/MRI datasets allowed for a correct N-staging in 8 (80 %) of the 10 patients. In addition, five patients comprised inguinal and/or paraaortic lymph node metastases (defined as M1-stage), based on the reference standard. PET/MRI permitted correct detection of all five patients with nonregional metastatic lymph nodes from cervical cancer. Moreover, no other distant metastases were present.

Quantitative analysis

To investigate potential correlations of quantitative parameters in PET/MRI depending on tumor histology and/or prognostic factors of cervical cancer (tumor stage, differentiation grade, tumor size, nodal status), mean values for SUV and ADC of all assessed tumor lesions were calculated (Table 4). The mean size of all primary cervical cancer lesions amounted to 39.8± 25.9 mm. Mean SUVs for all assessed primary cervical cancers exhibited a significant correlation with tumor size, whereas calculated ADC values revealed an inverse correlation with the size of tumor lesions of the uterine cervix (Fig. 3). Determined SUVs for poorly-differentiated tumors were significantly higher ($p < 0.05$) than for well- and moderately-differentiated cancer lesions (Fig. 4). In addition, poorly-

Table 3 Sensitivity and specificity for the determination of local tumor extent in PET/MRI

	Sensitivity	Specificity
Invasion of vagina	82 % (9/11) (95 % CI: 48–98 %)	94 % (15/16) (95 % CI: 70–100 %)
Invasion of parametrium	90 % (9/10) (95 % CI: 55–100 %)	94 % (16/17) (95 % CI: 71–100 %)
Invasion of pelvic sidewall	100 % (3/3)	100 % (24/24)
Invasion of bladder/rectum	100 % (2/2)	100 % (25/25)

Fig. 2 Images of a 31-year-old patient with primary cervical cancer and a para-aortic lymph node metastasis (**a**, *arrow*), which shows high signal intensity in DWI (**b**; b-1000). Correlating PET (**c**) reveals a focally increased FDG-uptake which corresponds to the lymph node on fused PET/MR images (**d**)
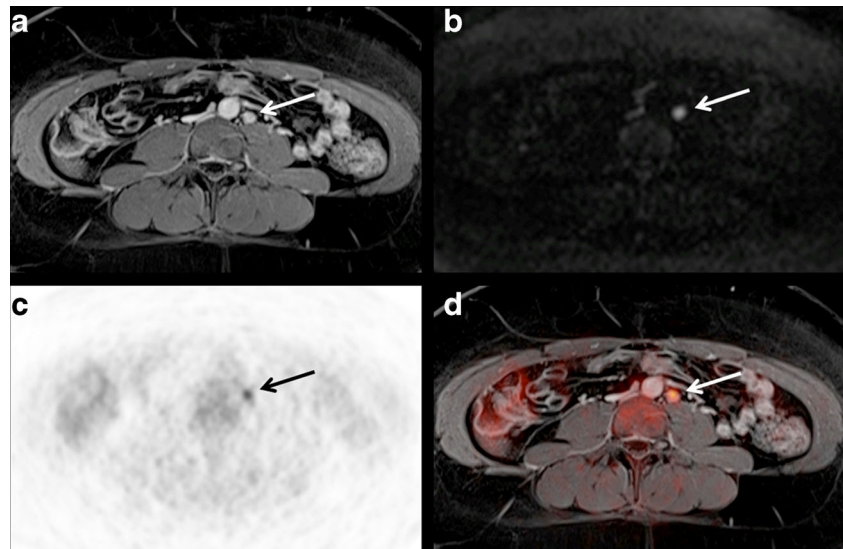

Table 4 Calculated mean values of PET/MRI derived SUVs and ADC values for all tumor lesions as well as in dependence of tumor histology and prognostic factors of cervical cancer

	Category	No. of patients	SUVmax	SUVmean	ADCmean (x10⁻³ mm²/s)	ADCmin (x10⁻³ mm²/s)
Primary cancers	All tumors	27	12.5±6.1	6.1±2.7	1.11±0.17	0.61±0.17
Histological type	Squamous cell carcinoma	22	13.0±6.4	6.3±2.8	1.11±0.18	0.61±0.18
	Adenocarcinoma	5	10.3±4.4	5.4±2.1	1.09±0.12	0.61±0.13
			(0.417)	(0.421)	(0.755)	(0.901)
Tumor grade	G1+G2	17	10.1±5.4	5.0±2.2	1.15±0.17	0.67±0.17
	G3	10	16.7±5.0	8.0±2.4	1.04±0.13	0.51±0.11
			(0.005)	(0.002)	(0.079)	(0.014)
T-stage	IB/IIA	16	12.2±6.9	6.0±3.0	1.15±0.18	0.66±0.17
	IIB/IIIB/IV	11	13.1±5.0	6.3±2.2	1.05±0.14	0.52±0.14
			(0.521)	(0.490)	(0.145)	(0.043)
Nodal status	Nodal negative	16	11.5±6.1	5.6±2.5	1.13±0.17	0.65±0.18
	Nodal positive	11	14.0±6.0	6.9±2.9	1.07±0.15	0.53±0.12
			(0.236)	(0.245)	(0.300)	(0.061)
Tumor size	<4 cm	19	10.3±5.4	5.2±2.3	1.15±0.16	0.66±0.16
	>4 cm	8	17.9±4.0	8.2±2.2	1.01±0.14	0.47±0.10
			(0.004)	(0.002)	(0.019)	(0.001)

P values are presented within brackets. Furthermore, significant differences between SUV and ADC values ($p<0.05$) are marked within the table (square bracket)
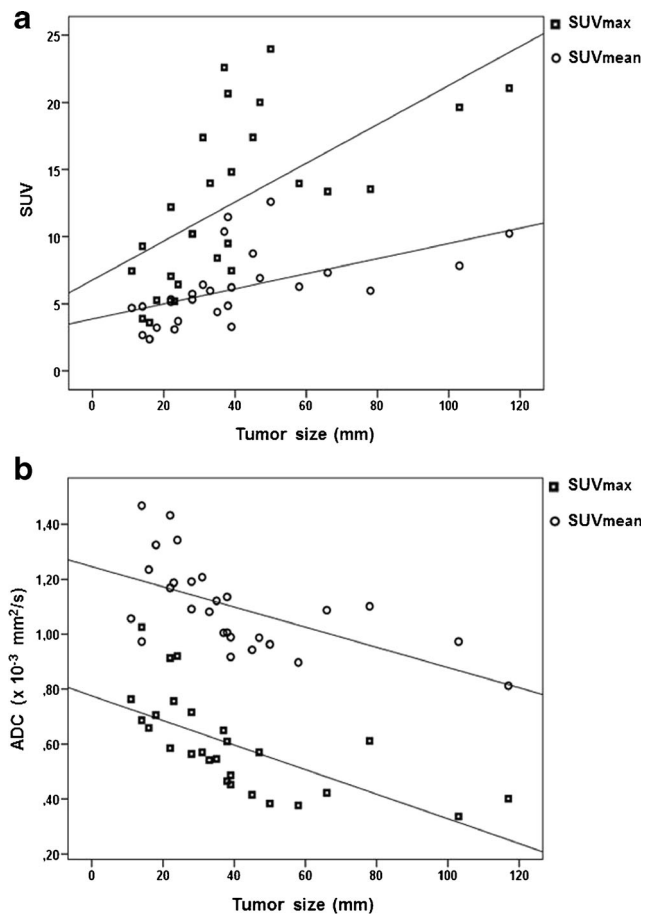
Fig. 3 Scatter plots showing a significant correlation between tumor size and SUVs (**a**) as well as an inverse correlation between the size of primary tumors of the uterine cervix and determined ADC values (**b**)

differentiated cancers showed significantly ($p<0.05$) lower ADCmin values when compared to well- and moderate-differentiated tumors. No significant differences could be obtained for SUVs between patients with early (stage IB-IIA) or advanced (stage IIB-IVA) tumor stages, whereas significantly lower ADCmin values were detected for primary cervical cancers with advanced tumor stages. In addition, obtained SUV or ADC values did not show a significant correlation with tumor histology and nodal status.

Discussion

The present study investigated the diagnostic utility of integrated PET/MRI for a pretreatment diagnostic work-up of patients with primary cervical cancer. PET/MRI enabled the correct detection of all primary tumors of the uterine cervix, yielded correct identification of the T-stage in 85 % of the cases, and offered 91 % sensitivity and 94 % specificity rates for the identification of nodal-positive patients. Furthermore, PETMRI offered additional simultaneous analysis of

functional parameters, revealing significant correlations between SUV and ADC values to tumor size and differentiation grade.

As prognosis, in terms of tumor recurrence and mortality, of cervical cancer is dependent on tumor spread at initial diagnosis, highly accurate tumor staging is mandatory to ensure best patient management. Staging of cervical cancer is based on three cornerstones, by means of local T-staging, nodal staging (N-staging) as well as potential distant metastases (M-staging). According to the recommendations of the FIGO staging system, cervical cancers are primarily staged by clinical evaluation [2]. Nevertheless, cross-sectional imaging has been shown to be more precise in the assessment of tumor invasion into adjacent anatomical structures, with MRI revealing its superiority over other conventional imaging modalities [17, 18]. MR imaging has been demonstrated very accurate for the detection of parametrial invasion and the exclusion of bladder or rectal invasion, representing two important determinants for the correct selection of the appropriate initial treatment [5]. With increasing introduction of hybrid imaging techniques for oncologic imaging, PET/CT and PET/MRI have become the focus of interest in the past years for the evaluation of gynecological cancers [19]. A recent publication by Kitajima et al. investigated the diagnostic value of retrospectively fused PET and MRI datasets for T- and N-staging of primary cervical cancers [20]. Their results showed an identical overall accuracy for fused PET/MRI and contrast-enhanced MRI (83.3 %) examinations for T-staging, with significantly higher values when compared to PET/CT (53.3 %) due to the inferior soft-tissue-contrast of the CT component. Our study results support these findings, showing the high diagnostic capacity of PET/MRI for the assessment of primary tumor lesions as well as tumor infiltration into adjacent soft tissue. Yet, while sensitivity rates for tumor infiltration of the pelvic sidewall and bladder/rectum amounted to 100 %, microscopic infiltration of the vagina remained undetected in 2 patients based on PET/MRI and parametrial invasion was misclassified in two further patients, focally degrading the overall sensitivity rates in our study.

Apart from determining the local tumor spread, the detection of potential lymph node metastases at initial diagnosis is considered an additional strong predictor for prognosis of cervical cancer patients [21]. Hybrid imaging, in terms of PET/CT, has been shown highly beneficial and superior to conventional imaging techniques for lymph node staging in numerous tumor entities [15, 22]. First studies on retrospectively fused PET/MRI showed identical results for sensitivity (92.3 %), specificity (88.2 %) and accuracy (90.0 %) for the identification of lymph node metastases in comparison to PET/CT, but higher values than MRI alone (69.2 %, 100 % and 86.7 %) [20]. In a region-based approach, Kim et al. evaluated the diagnostic potential of retrospectively fused PET/MRI for nodal staging of cervical cancer patients in comparison to PET/CT [23]. The authors

Fig. 4 Poorly-differentiated tumors (G3) of the uterine cervix showed significantly higher SUVs than well- and moderately-differentiated (G1 + G2) cancers (**a**). In addition, determined ADCmin values were significantly lower for poorly-differentiated tumors than for well- and moderately-differentiated tumors, whereas calculated values for ADCmean (hatched) showed only a tendency but the differences missed significance level (**b**)
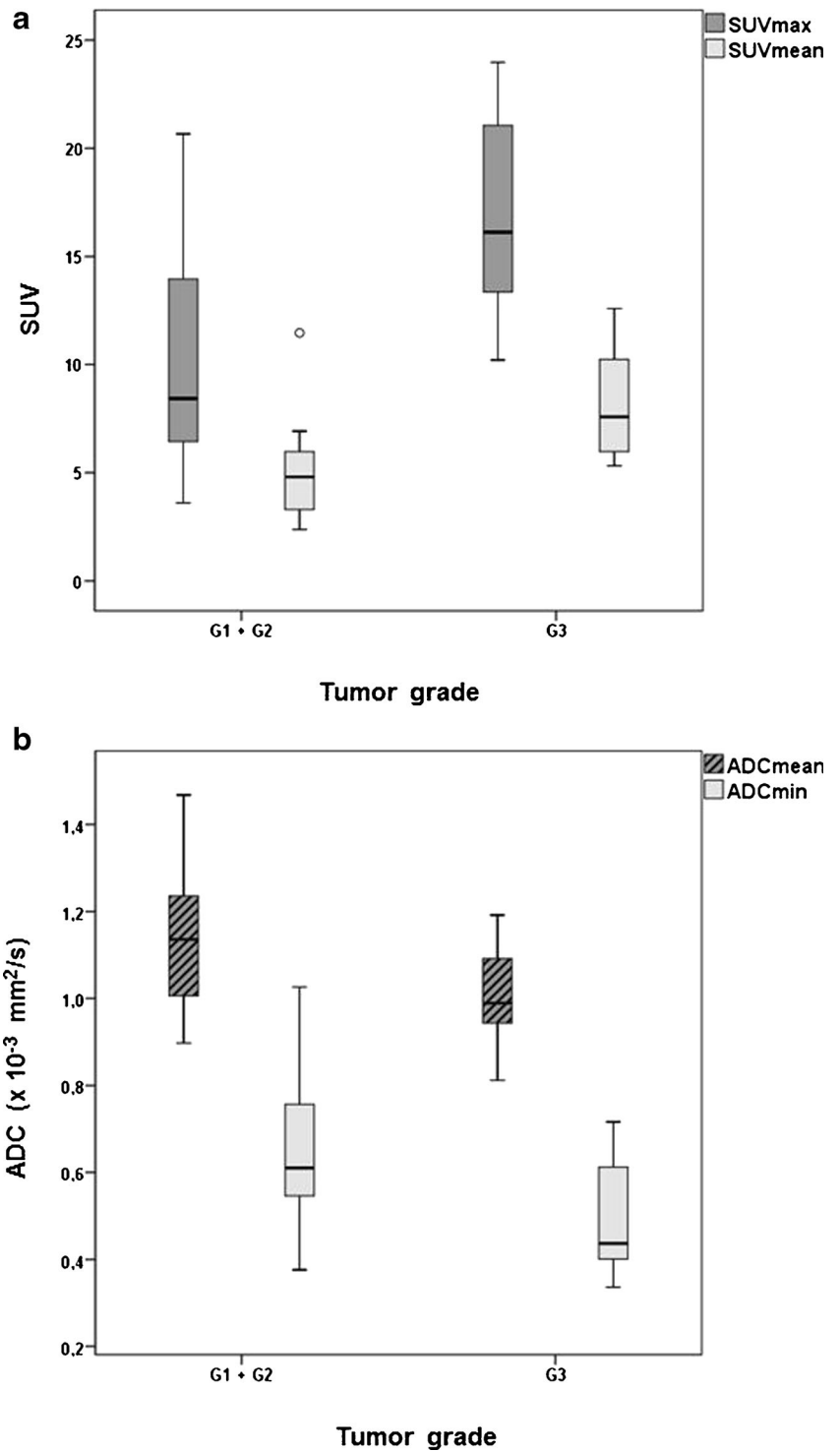
reported slightly significantly better results for the detection of pelvic and para-aortic lymph node metastases in ratings performed on fused PET/MRI images over PET/CT. Initial studies on simultaneous PET/MRI underline the aforementioned results, in demonstrating superior lymph node metastases detection based on PET/MRI over MRI alone, whereas comparable results have been shown between simultaneous PET/MRI and

PET/CT [24, 25]. In accordance with these findings, our results support the high diagnostic value of PET as part of hybrid imaging, thus offering an accurate nodal staging of cervical cancer patients with sensitivity rates of 91 % and specificity rates of 94 %.

In addition to morphologic staging, functional parameters have been demonstrated to offer valuable prognostic

information in oncological patients [26, 27]. Integrated PET/MRI systems enable the simultaneous acquisition of morphological and functional datasets in a single imaging session (Fig. 5), offering highly-accurate co-registration accompanied by a reduction of motion and misregistration artifacts. A recently presented study showed the successful use of further radiotracers (e.g., 18F-Fluoromisonidazole, determining hypoxic tumor areas) for the evaluation of primary cervical cancers [28]. Accordingly, multiparametric PET/MR imaging might enable a better understanding of tumor biology and could be utilized for an improved therapy planning and treatment monitoring. Although tumor detection and characterization of PET and DWI are based on different aspects of tumor biology, both functional parameters have been considered to be prognostic predictors for patients with cervical cancer [13, 29]. In a study of 66 patients, Nakamura et al. investigated an association of subsequently obtained SUV and ADC values with cervical cancer-related features [13]. Their results showed shorter disease-free and overall survival rates in cervical cancer lesions exhibiting higher SUVmax combined with lower ADCmin values. Furthermore, the authors reported a significant correlation of a higher SUVmax with higher tumor stage, larger primary tumor lesion and the occurrence of lymph node metastases. In accordance with the results of Nakamura et al., our study results also demonstrated a significant correlation between SUV and ADC values and the tumor size and differentiation grade. Furthermore, the present study illustrates that poorly-differentiated tumors exhibit higher SUVs and lower ADCmin values in comparison to well- and moderately differentiated cervical tumor lesions. Investigating variations in glucose metabolism of cervical cancers in

dependence of differentiation levels, Kidd et al. published similar results, showing a significant higher FDG uptake in poorly-differentiated compared to well-differentiated tumors [30]. Our results regarding the ADC values go in line with a recent publication, in demonstrating the correlation between lower ADC values and poorly differentiated tumors compared to those that were well- or moderately differentiated [31]. Hence, considering both tumor grade dependent functional parameters, integrated PET/MRI enables the assessment of two biomarkers that may be used for non-invasive prediction of tumor aggressiveness and prognostic appraisal.

Investigating these first steps of integrated PET/MRI for primary staging of cervical cancer patients, our study is not free of limitations. Based on the rather small study population, our results should be considered preliminary and open for further confirmation. In addition, exclusive PET/MR imaging was performed, since PET/CT has not been proven useful as a stand-alone technique for primary staging of cervical cancer patients. Comparative studies, evaluating the accuracy of these two imaging modalities (especially focusing on nodal staging), would be of interest. Furthermore, in this exploratory study multiple testing was performed to indicate potential differences between SUV and ADC values of primary tumors in dependence of main prognostic factors of cervical cancer. Due to the small case number, differences between the determined values have to be considered as a tendency and must be confirmed by the use of larger patient cohorts in future studies.

Fig. 5 Thirty-three-year-old patient with a poorly-differentiated cervical cancer (stage Ib). Axial T1w VIBE imaging (a) shows a contrast-enhancing mass of the uterine cervix, revealing an extensive focal FDG accumulation on PET/MR images (b). The identical tumor lesion shows high signal in DWI (c; b-1000) with a signal drop in corresponding ADC map (d)
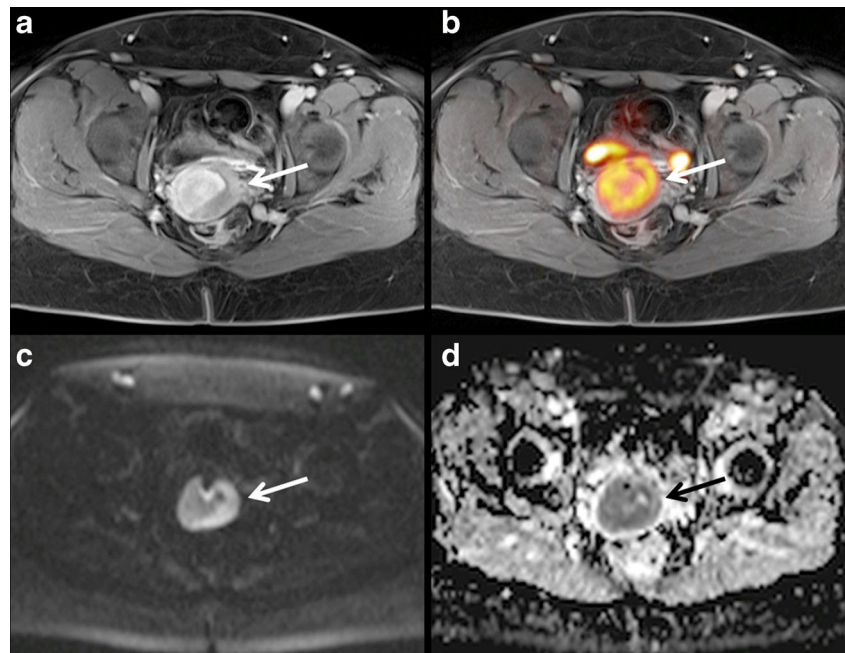
Conclusions

In Conclusion our initial study results demonstrate the high diagnostic performance of integrated PET/MRI for dedicated primary local tumor and nodal staging of patients with cervical cancer. In addition, PET/MRI offers the simultaneous acquisition of two functional biomarkers for tumor aggressiveness and patient prognosis. Therefore, integrated PET/MRI bears the potential to be applied as a valuable alternative/adjunct for the clinical work-up of cervical cancer patients in a pretreatment setting.

References

1. Jemal A, Bray F, Center MM, Ferlay J, Ward E, Forman D. Global cancer statistics. CA Cancer J Clin. 2011;61:69–90.
2. Quinn MA, Benedet JL, Odicino F, Maisonneuve P, Beller U, Creasman WT, et al. Carcinoma of the cervix uteri. FIGO 26th Annual Report on the Results of Treatment in Gynecological Cancer. Int J Gynaecol Obstet. 2006;95 Suppl 1:S43–S103.
3. Lagasse LD, Creasman WT, Shingleton HM, Ford JH, Blessing JA. Results and complications of operative staging in cervical cancer: experience of the Gynecologic Oncology Group. Gynecol Oncol. 1980;9:90–8.
4. Freeman SJ, Aly AM, Kataoka MY, Addley HC, Reinhold C, Sala E. The revised FIGO staging system for uterine malignancies: implications for MR imaging. Radiographics. 2012;32:1805–27.
5. Sala E, Wakely S, Senior E, Lomas D. MRI of malignant neoplasms of the uterine corpus and cervix. AJR Am J Roentgenol. 2007;188:1577–87.
6. Havrilesky LJ, Kulasingam SL, Matchar DB, et al. FDG-PET for management of cervical and ovarian cancer. Gynecol Oncol. 2005;97:183–91.
7. Antoch G, Saoudi N, Kuehl H, Dahmen G, Mueller SP, Beyer T, et al. Accuracy of whole-body dual-modality fluorine-18-2-fluoro-2-deoxy-D-glucose positron emission tomography and computed tomography (FDG-PET/CT) for tumor staging in solid tumors: comparison with CT and PET. J Clin Oncol. 2004;22:4357–68.
8. Bar-Shalom R, Yefremov N, Guralnik L, Gaitini D, Frenkel A, Kuten A, et al. Clinical performance of PET/CT in evaluation of cancer: additional value for diagnostic imaging and patient management. J Nucl Med. 2003;44:1200–9.
9. Wetter A, Lipponer C, Nensa F, Beiderwellen K, Olbricht T, Rubben H, et al. Simultaneous 18F choline positron emission tomography/magnetic resonance imaging of the prostate: initial results. Investig Radiol. 2013;48:256–62.
10. Pace L, Nicolai E, Luongo A, Aiello M, Catalano OA, Soricelli A, et al. Comparison of whole-body PET/CT and PET/MRI in breast cancer patients: lesion detection and quantitation of 18F-deoxyglucose uptake in lesions and in normal organ tissues. Eur J Radiol. 2014;83:289–96.
11. Heusch P, Buchbender C, Kohler J, Nensa F, Beiderwellen K, Kuhl H, et al. Correlation of the apparent diffusion coefficient (ADC) with the standardized uptake value (SUV) in hybrid 18F-FDG PET/MRI in non-small cell lung cancer (NSCLC) lesions: initial results. Röfo. 2013;185:1056–62.
12. Elmi A, Hedgire SS, Covarrubias D, Abtahi SM, Hahn PF, Harisinghani M. Apparent diffusion coefficient as a non-invasive predictor of treatment response and recurrence in locally advanced rectal cancer. Clin Radiol. 2013;68:e524–31.
13. Nakamura K, Joja I, Kodama J, Hongo A, Hiramatsu Y. Measurement of SUVmax plus ADCmin of the primary tumour is a predictor of prognosis in patients with cervical cancer. Eur J Nucl Med Mol Imaging. 2012;39:283–90.
14. Shanmugan S, Arrangoiz R, Nitzkorski JR, Yu JQ, Li T, Cooper H, et al. Predicting pathological response to neoadjuvant chemoradiotherapy in locally advanced rectal cancer using 18FDG-PET/CT. Ann Surg Oncol. 2012;19:2178–85.
15. Antoch G, Stattaus J, Nemat AT, Marnitz S, Beyer T, Kuehl H, et al. Non-small cell lung cancer: dual-modality PET/CT in preoperative staging. Radiology. 2003;229:526–33.
16. Kitajima K, Murakami K, Yamasaki E, Domeki Y, Kaji Y, Morita S, et al. Performance of integrated FDG-PET/contrast-enhanced CT in the diagnosis of recurrent uterine cancer: comparison with PET and enhanced CT. Eur J Nucl Med Mol Imaging. 2009;36:362–72.
17. Subak LL, Hricak H, Powell CB, Azizi L, Stern JL. Cervical carcinoma: computed tomography and magnetic resonance imaging for preoperative staging. Obstet Gynecol. 1995;86:43–50.
18. Sala E, Rockall AG, Freeman SJ, Mitchell DG, Reinhold C. The added role of MR imaging in treatment stratification of patients with gynecologic malignancies: what the radiologist needs to know. Radiology. 2013;266:717–40.
19. Lee SI, Catalano OA, Dehdashti F. Evaluation of gynecologic cancer with mr imaging, 18F-FDG PET/CT, and PET/MR imaging. J Nucl Med. 2015;56:436–43.
20. Kitajima K, Suenaga Y, Ueno Y, Kanda T, Maeda T, Deguchi M, et al. Fusion of PET and MRI for staging of uterine cervical cancer: comparison with contrast-enhanced (18)F-FDG PET/CT and pelvic MRI. Clin Imaging. 2014;38:464–9.
21. Tanaka Y, Sawada S, Murata T. Relationship between lymph node metastases and prognosis in patients irradiated postoperatively for carcinoma of the uterine cervix. Acta Radiol Oncol. 1984;23:455–9.
22. Veit P, Ruehm S, Kuehl H, Stergar H, Mueller S, Bockisch A, et al. Lymph node staging with dual-modality PET/CT: enhancing the diagnostic accuracy in oncology. Eur J Radiol. 2006;58:383–9.
23. Kim SK, Choi HJ, Park SY, Lee HY, Seo SS, Yoo CW, et al. Additional value of MR/PET fusion compared with PET/CT in the detection of lymph node metastases in cervical cancer patients. Eur J Cancer. 2009;45:2103–9.
24. Grueneisen J, Beiderwellen K, Heusch P, Gratz M, Schulze-Hagen A, Heubner M, et al. Simultaneous positron emission tomography/magnetic resonance imaging for whole-body staging in patients with recurrent gynecological malignancies of the pelvis: a comparison to whole-body magnetic resonance imaging alone. Invest Radiol. 2014;49:808–15.

25. Heusch P, Nensa F, Schaarschmidt B, Sivanesapillai R, Beiderwellen K, Gomez B, et al. Diagnostic accuracy of whole-body PET/MRI and whole-body PET/CT for TNM staging in oncology. Eur J Nucl Med Mol Imaging. 2015;42:42–8.

26. Song BI, Lee SW, Jeong SY, Chae YS, Lee WK, Ahn BC, et al. 18F-FDG uptake by metastatic axillary lymph nodes on pretreatment PET/CT as a prognostic factor for recurrence in patients with invasive ductal breast cancer. J Nucl Med. 2012;53:1337–44.

27. Fujimoto H, Kazama T, Nagashima T, Sakakibara M, Suzuki TH, Okubo Y, et al. Diffusion-weighted imaging reflects pathological therapeutic response and relapse in breast cancer. Breast Cancer. 2014;21:724–31.

28. Pinker-Domenig K, Baltzer P, Magometschnigg H, Polanec S, Andrezejewski P, Sturdza AE, et al. PET/MRI in cervical cancer: insights into tumor biology. J Clin Oncol. 2015;33:(suppl; abstr 5597).

29. Kidd EA, Siegel BA, Dehdashti F, Grigsby PW. The standardized uptake value for F-18 fluorodeoxyglucose is a sensitive predictive biomarker for cervical cancer treatment response and survival. Cancer. 2007;110:1738–44.

30. Kidd EA, Spencer CR, Huettner PC, Siegel BA, Dehdashti F, Rader JS, et al. Cervical cancer histology and tumor differentiation affect 18F-fluorodeoxyglucose uptake. Cancer. 2009;115:3548–54.

31. Kuang F, Ren J, Zhong Q, Liyuan F, Huan Y, Chen Z. The value of apparent diffusion coefficient in the assessment of cervical cancer. Eur Radiol. 2013;23:1050–8.